Nanoscale

Accepted Manuscript

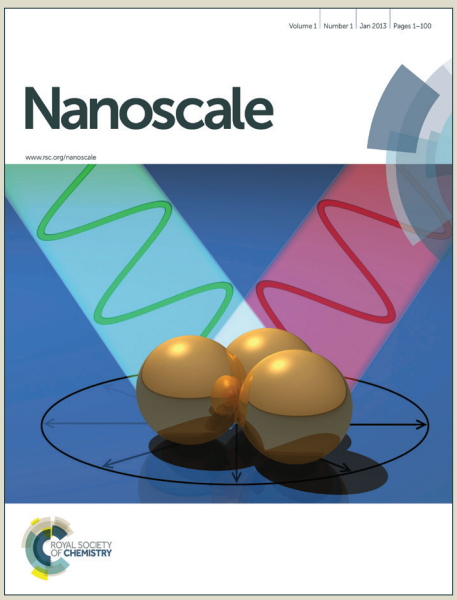

ROYAL SOCIETY OF CHEMISTRY

www.rsc.org/nanoscale

Nanoscale

RSCPublishing

ARTICLE

Cascading Electron and Hole Transfer Dynamics in CdS/CdTe Core-Shell Sensitized Bromo-Pyrogallol Red (Br-PGR): Slow Charge Recombination in Type II Regime

Cite this: DOI: 10.1039/xoxxoooooox

Received ooth September 2014,
Accepted ooth 2014

DOI: 10.1039/xoxxoooooox

www.rsc.org/nanoscale

Partha Maity, Tushar Debnath, Uday Chopra and Hirendra Nath Ghosh*

Abstract

Ultrafast cascading hole and electron transfer dynamics has been demonstrated in CdS/CdTe type II core/shell sensitized with Br-PGR using transient absorption spectroscopy and the charge recombination dynamics has been compared with CdS/Br-PGR composite materials. Steady state optical absorption studies suggest that Br-PGR form strong charge transfer (CT) complex with both CdS QD and CdS/CdTe core-shell. Hole transfer from photo-excited QD and QD core-shell to Br-PGR was confirmed by both steady state and time-resolved emission spectroscopy. Charge separation was also confirmed by detecting electron in the conduction band of QDs and cation radical of Br-PGR as measured from femtosecond transient absorption spectroscopy. Charge separation in CdS/Br-PGR composite materials was found to take place in three different pathways, by transferring the photoexcited hole of CdS to Br-PGR, electron injection from photoexcited Br-PGR to the CdS QD, and direct electron transfer from the HOMO of Br-PGR to the conduction band of the CdS QD. However in CdS/CdTe/Br-PGR system hole transfer from photo-excited CdS to Br-PGR and electron injection from photo-excited Br-PGR to CdS take place after cascading through CdTe shell QD. Charge separation also takes place via direct electron transfer from Br-PGR HOMO to the conduction band of CdS/CdTe. Charge recombination (CR) dynamics between electron in conduction band of CdS QD and Br-PGR cation radical was determined by monitoring the bleach recovery kinetics. CR dynamics was found to be much slower in CdS/CdTe/Br-PGR system as compared to that in CdS/Br-PGR system. Formation of strong CT complex and separation of charges cascading through the CdTe shell help to slow down the charge recombination in the type II regime.

Introduction

Design and development of quantum-dot-sensitized solar cells (QDSSCs) has drawn considerable research attention due of their conceptual similarities with dye-sensitized solar cells (DSSCs) and the outstanding opto-electronic properties of quantum dot sensitizers[1–7]. It is believed that single photon can generate more than one electron-hole pair on photoexcitation of quantum dot due to multiple exciton generation (MEG)[8-10] , which intern can drastically increase the efficiency of the devices. However it is important to dissociate multiple exciton before ultrafast exciton-exciton annihilation which take place in fast and ultrafast time scale in most of the QD materials[11-14]. Till date the efficiency of the QD based solar cell has not reached to double numerical figure[15-17] where as DSSC has reached 13% efficiency using porphyrin based sensitizer molecule with Co (II/III) redox shuttle electrolyte[18]. Lower conversion efficiency in QDSC observed are due to many reasons like limited absorption of the QDs in incident light, slow hole transfer rate ensuing photo anode corrosion. In addition to that lower QD loading on TiO_2 surface (as compared to dye loading in DSSC) resulting direct electron transfer from TiO_2 film to the oxidized redox couple in photo anode. It has been realized that it is important to extract both electron and hole from photo-excited QD before ultrafast exciton-exciton annihilation[19]. Electron injection is much faster as compared to hole transfer, so for efficient devices hole has to extracted from QD surface as fast as possible[20]. By introducing molecular adsorbate on QD surface it is possible to extract the hole where the HOMO level of molecular adsorbate lies above the valence band of the quantum dots. In addition to hole extraction the same molecular adsorbate can also inject electron to QD on photoexcitation which can act as co-sensitizer absorbing light in the red region of solar spectrum.

To improve the conversion efficiency in QD solar cell, it is necessary to dissociate the photo-excited exciton through electron or hole extraction before they recombine. Exciton dissociation through electron transfer in QD/TiO_2[21-23] and QD/molecular adsorbate[24-25] systems have been widely investigated which mostly take place in fast and ultrafast time scale. However exciton dissociation through hole transfer is not widely reported in literature except few recent reports by us [26-29] and Kamat & co-workers[30]. Electron extraction

from quantum dot can be as fast as sub-100 fs however hole transfer from phto-excited QD to molecular adsorbate can be as slow as 500-800 fs as we have reported in CdS/DBF[26] and CdSe/PGR[27] composite materials. Interestingly both the composite materials[26,27] realized to be suitable for super-sensitizer due to higher charge separation and slower charge recombination. However instead of pure QDs, sometime core/shell QDs are used as a photo anode in QDSC for better performance. Many authors have used type II core-shell[31-41] quantum dot materials as compared to pure QD to improve conversion efficiency in QDSC[42-43], due to higher charge separation in type II band alignment for the QD materials. Introducing a molecular adsorbate with type-II core-shell it is possible to improve further charge separation where both photo-excited QD and molecular adsorbate actively take part in charge separation process. Charge transfer dynamics in quantum dot core-shell involving molecular adsorbate are reported in the literature, where in most of the cases electron transfer dynamics has been discussed[44-47]. However no reports are available where hole transfer play active role in charge separation in type II core-shell sensitized molecular adsorbate. To improve any kind of device efficiency using type II core-shell and molecular adsorbate it is very important to understand charge transfer dynamics in ultrafast time scale where both electron and hole transfer processes are involve.

Herein we have demonstrated and compared charge transfer dynamics in CdS QD and CdS/CdTe type II core-shell sensitized by bromo-pyrogallol red (Br-PGR) in fast and ultrafast time scale using time-resolved emission and Femto-second time-resolved absorption techniques. Redox energy levels of the CdS QD and Br-PGR molecule imply that the HOMO (highest occupied molecular orbital) and LUMO (lowest unoccupied molecular orbital) levels of the Br-PGR molecule lies energetically above the valence band (VB) and conduction band (CB) of CdS QD and CdS/CdTe core-shell. In the composite materials photo-excited Br-PGR can inject electron into both CdS QD and CdS/CdTe core-shell and Br-PGR also can extract hole from photo-excited CdS QD and CdS/CdTe core-shell. Effect of shell on both electron injection and hole transfer dynamics in CdS/CdTe type II core shell and also charge recombination dynamics has been demonstrated in the present investigation. To the best of our knowledge we are reporting for the first time cascade electron injection and hole transfer dynamics in CdS/CdTe type II core-shell-sensitized by molecular adsorbate. We have also discussed the feasibility of using these quantum dot-molecular adsorbate composite materials as super-sensitizer in QD solar cell.

Experimental Section:

a) Materials: Bromo-pyrogallol red (Br-PGR) was obtained from Aldrich and used as a sensitizer molecule. Cadmium oxide (CdO, Aldrich), oleic acid (OA, Aldrich), trioctylphosphine (TOP, Aldrich, 90%), 1- octadecene (ODE, Aldrich) and sulphur powder (Aldrich) were used to prepare CdS QD. Methanol (AR) and chloroform (AR) were used as precipitation and re-dissolved the QD respectively. Finally all measurements were done in chloroform (Aldrich) solution and ethyl acetate (Aldrich) for TA measurement of pure Br-PGR.

b) Preparation of CdS QD: Oleic acid caped CdS QD was synthesized after following previously available literature method[48]. In brief; a stock cadmium oleate solution was prepared by heating a mixture of 3.4ml oleic acid (10.6 mmol), 0.51 g cadmium oxide (4.0 mmol) and 11.6 ml octadecene in a three-neck round-bottom flask at 180 °C in inert atmosphere (Ar). Solution became colorless and sulphur solution was swiftly injected through a syringe to the reaction mixture at 310 °C. Temperature of the mixture was reduced to 20 °C and growth of CdS QD monitored at 280 °C. To prepare the sulpher solution, 0.064 g of sulpher powder (2 mmol) was mixed with 1.1 ml TOP (2.5mmol). The resulting colorless solution was obtained in 4.4 ml octadecene to give a final stock solution volume of 5.5 mL. Typically rapid color changes from pale-yellow to dark fluorescent yellow color were observed. The solution was dissolved with chloroform and then re-precipitated with methanol for 3 times at room temperature.

c) Preparation of CdS-CdTe core-shell:

To synthesize CdS/CdTe type II core-shell, prepared (as described earlier) CdS QD solution in chloroform was directly used as core. CdTe shell on CdS QD was prepared by using Cd-oleate as cadmium precursor and tellurium precursor as tellurium precursor. Cd-oleate was prepared by adding 0.112 g of CdO (0.876 mmol) and 0.74 ml oleic acid (2.3 mmol) in 2.5 ml octadecene under reflux condition (at 180°C) into a three-neck round bottom flask in inert atmosphere. This Cd-oleate was added to a 1 μmole CdS solution in a three-neck round bottom flask. The mixture of 0.112 g Te (0.876 mmol), 0.5 ml TOP (1.09 mmol) and 10 ml octadecene was dropwise added to the solution through a syringe at 180°C. Finally the reactant solution was dissolved with chloroform and re-precipitated with methanol for 3 times.

d) Steady State Optical Absorption and Emission Spectrometer:

Steady-state absorption spectra were recorded on a Thermo-Electron model Biomate spectrophotometer. Fluorescence spectra, which were corrected for the wavelength dependence of the instrument sensitivity, were recorded using Hitachi model 4010 Spectrofluorometer.

e) Time Resolved Emission Spectrometer:

Time resolved fluorescence measurements were carried out using a diode laser based spectrofluorimeter from IBH (UK). The instrument works on the principle of time-correlated single photon counting (TCSPC). In the present work, a 374 nm, 406 nm laser pulses were used as the excitation light sources and a TBX4 detection module (IBH) coupled with a special Hamamatsu PMT was used for fluorescence detection.

f) Femtosecond Transient Absorption Studies:

Ultrafast transient absorption measurements were carried out in femtosecond (0.1 ps-4 ns) transient absorption (TA) spectrometer which is based on multi-pass Ti: sapphire laser system (CDP, Moscow, 800 nm, <100 fs, 1.2 mJ/pulse, and 1 kHz repetition rate) and Excipro pump-probe spectrometer (CDP, Moscow). Briefly the pulses of 40 fs duration and 4 nJ energy per pulse at 800 nm obtained from a self-mode-locked Ti-Sapphire laser oscillator (Tissa 50, CDP, Moscow, Russia) were amplified in a multi-pass amplifier pumped by a 20W DPSS laser (Jade-II, Thales Laser, France) to generate 40 fs laser pulses of about 1.2 mJ energy at a repetition rate of 1 kHz. Pump pulse at 400 nm were generated by frequency doubling of the 800 nm pulse at a β-barium borate (BBO) crystal. To generate visible probe pulses (from 450 to 850 nm), about 1 μJ of the 800 nm beam is focused onto a 3 mm thick sapphire window and splitting into a probe and reference beam. The spectrometer is coupled with Multi channel detector head, with two 1024-pixels linear image sensors, 200 -1000 nm spectral response (10% of peak), up to 1 kHz readout rep rate. An imaging spectrometer is adapted to the detector head and connected to a computer via serial port with

Visible grating 300 –1100 nm spectral range which has 206 nm detection range. The pump beam diameter at the sample is ~350 µm, corresponding to an excitation density of 0.28 µJ/cm^2. The probe beam was focused with an Al parabolic reflector onto the sample (with a beam diameter of 150 µm at the sample). The instrument response function (IRF) for 400 nm excitation was obtained by fitting the rise time of the bleach of sodium salt of *meso* tetrakis (4 sulfonatophenyl) porphyrin (TPPS) at 710 nm and found to be 120 fs. The <N>(jσ) was maintained <1 to prevent multiexciton formation due to higher pump intensity. For all spectroscopy measurements, the samples were kept in a 1 mm cuvette and the experimental solutions were circulated to avoid sample bleaching during the course of the experiment. The data analysis and fitting at individual wavelengths were carried out by Lab-View program.

g) High resolution Transmission Electron Microscope Measurements:

High-resolution TEM (HRTEM) measurements were carried out using a JEOL–JEM-2010 UHR instrument operated at an acceleration voltage of 200 kV with a lattice image resolution of 0.14 nm. We have dissolved CdS QD and CdS/CdTe core-shell in chloroform to take TEM images. A drop of sample is added to the TEM grid (200 Mesh Size Holey Carbon coated Cu Grid). The sample on the grid is heated in oven for 1/2 h at 40ºC to remove the excess chloroform.

h) X-ray diffraction (XRD) measurements:

X-ray diffraction (XRD) measurements were carried out for both CdS and CdS/CdTe core-shell QDs to understand the crystalline nature of QD materials. Figure 1 shows XRD patterns of powdered precipitated fraction of CdS core and CdS/CdTe core-shell[34,41,49] (one monolayer shell). For CdS core all the peaks corresponding to 111, 220 and 311 planes matches exactly with wurtzite crystalline phase of CdS. However in case of CdS/CdTe core-shell XRD peaks due to both CdS wurtzite crystalline phase and CdTe zincblende crystalline phase appear in the XRD spectrum.

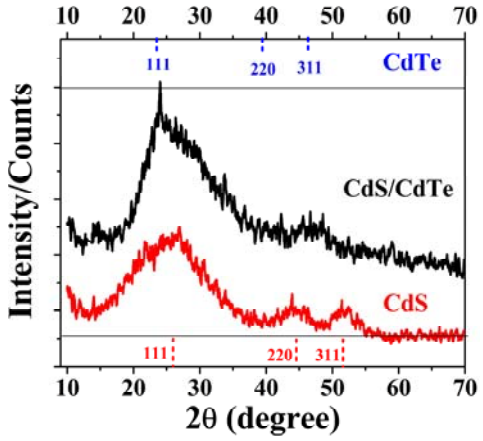

Figure 1: Measured powder X-ray diffraction (XRD) patterns of CdS core (red) and CdS/CdTe core/shell (black) nanocrystals QD. The vertical dotted bars at the bottom (red) and top (blue) of the figure show the reference planes of wurtzite CdS and zincblende CdTe nanocrystals respectively.

3. Results and Discussions:

a) Optical properties and characterization of the quantum dot core/shell:

After synthesizing both CdS QD and CdS/CdTe core-shell, we have carried out steady state optical absorption and emission properties and also measured the size of the particle by high resolution TEM. Figure 2 **(I)** (top panel) shows the optical absorption and emission spectra of CdS QD and Figure 2 **(II)** depicts the HRTEM image of that CdS QD. From steady state spectra it is clear that the first exciton of the QD appeared at 434 nm and the corresponding size was measured to be 2.5 nm from TEM image. Photoluminescence peak of CdS QD was observed to be 452 nm with emission quantum yield of 36% (details calculation are shown in supporting information) after exciting the QD at 375 nm and shown in Figure 2 (top panel, Figure 2 **I** trace "b"). We have also carried out time-resolved emission studies and average emission life time was found to be 12.7 ns and depicted in next section.

Figure 2 **(III)** (bottom panel) shows the optical absorption and emission spectra of CdS/CdTe core/shell QD and Figure 2 (**IV**) depicts the HRTEM image of synthesized CdS/CdTe core/shell. In optical absorption spectra one sharp peak appears at 436 nm and a broad absorption band appears in 500-600 nm regions. The absorption peak at 436 nm can be attributed to excitonic absorption due to CdS core and broad absorption band can be attributed to indirect band-gap transition in CdSe/CdTe type II core-shell. Size of the particle was determined to be 3.2 nm as measured from HRTEM studies (Supporting Information). Photoluminescence peak of CdS/CdTe core-shell was detected at 652 nm after exciting at 530 nm with relatively low emission quantum yield of 2.9% which is might be due to indirect band transition and also due to leaking of hole through surface induced non-radiative channels. Even after exciting CdS/CdTe core-shell at 374 nm, emission only due to indirect band transition at 652 nm was observed. At the same time we have also observed long emission lifetime at 652 nm due to indirect band gap emission of CdS/CdTe core-shell.

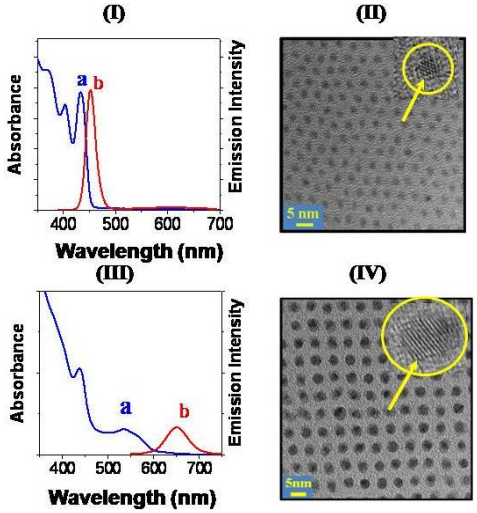

Figure 2: (I), **(III)** Optical absorption (a) and emission spectra (b) of CdS QD and CdS/CdTe core/shell respectively in chloroform solution. **(II), (IV)** The HRTEM image of CdS QD and CdS/CdTe respectively. Measured particle size of CdS and CdS/CdTe are 2.5 nm and 3.2 nm respectively (scale bar 5 nm). Lattice fringes for both the particles are shown in the inset of II and IV.

b) Charge transfer (CT) complex formation: Steady state optical absorption measurement

Main aim of the present investigation is to understand charge transfer behaviour in the excited state of CdS and CdS/CdTe

with Br-PGR composite materials and its applicability as a super sensitizer[50,26-30] in QDSC. In this circumstance it is very important to monitor the ground state interaction between QDs (both CdS QD and CdS/CdTe core-shell) and Br-PGR. Charge transfer interaction between quantum dot materials and molecular adsorbate are not widely reported in the literature except our report on di-bromo fluorescein (DBF) and CdS QD materials,where the composite materials form strong charge transfer complex[26]. In our earlier investigation[51]we have demonstrated that Br-PGR is one of the molecules in tri-phenyl methane series of dyes which can be potential sensitizer molecule in dye-sensitized solar cell (DSSC) where LUMO of Br-PGR lies above the conduction band of TiO_2. Figure 3A shows steady state optical absorption spectra of CdS QD (Figure 3a), Br-PGR (Figure 3b) and Br-PGR/CdS QD composite

(Figure 3c) in chloroform. Free Br-PGR shows optical absorption up to 650 nm with a peak at 480 nm which is attributed to lowest optical transition between HOMO and first excited state (S_1) of the Br-PGR molecule (Figure 3b). Interestingly on addition of Br-PGR in CdS solution, the color of the solution becomes deep blue (while the color of free Br-PGR and CdS are brown red and yellow respectively). The composite mixture shows broad absorption spectra (Figure 3c) in the entire visible region (beyond 750 nm) with a red shifted peak at 552 nm which indicates formation of strong charge transfer complex. We have also carried out steady state optical absorption studies of CdS/CdTe core-shell after sensitizing with Br-PGR. Figure 3 B shows the optical absorption spectra of CdS/CdTe (Figure 3d), Br-PGR (Figure 3e) and CdS/CdTe sensitized Br-PGR (Figure 3f). Optical absorption spectra of CdS/CdTe/Br-PGR composite mixture become much broader and red-shifted with absorption maxima at 570 nm.

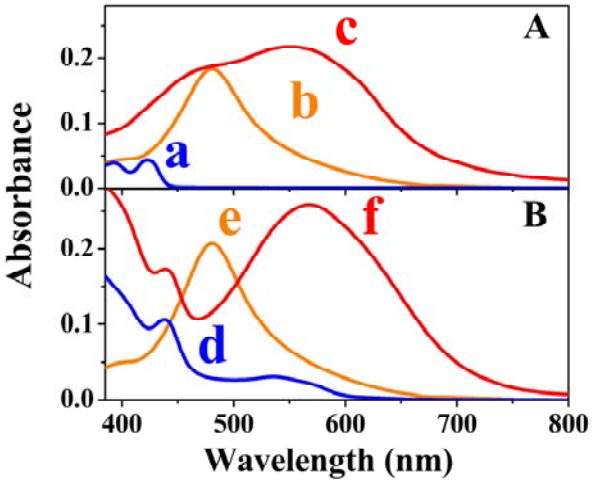

Figure 3: (A) Optical absorption spectra of (a) CdS QD (0.1μM), (b) Br-PGR (36μM) and (c) CdS QD sensitized PGR in chloroform. **(B)** Optical absorption spectra of (d) CdS/CdTe core/shell (0.1μM), (e) Br-PGR (b, 40μM) and (c) CdS/CdTe core-shell sensitized Br-PGR in chloroform.

A higher extinction coefficient of the QDs-Br-PGR composites suggest that Br-PGR form strong charge transfer complexes with both the QDs (CdS QD, CdS/CdTe type II core-shell) where partial charge transfer take place in the ground state. It is interesting to see that Br-PGR form better complex with CdS/CdTe type II core-shell as compared pure CdS QD. This observation clearly suggests that both the composite systems potential material for supersensitizer, which can absorb more solar radiation as compared to that of the individual QDs and Br-PGR molecule.

c) Hole Transfer Process: Photoluminescence (PL) measurement

From steady state optical absorption measurements we have observed that Br-PGR form strong CT complex with both CdS QD and CdS/CdTe type II core-shell. Now to understand charge transfer dynamics in the excited state in CdS/Br-PGR composite material steady state emission spectroscopy have been carried out by exciting Br-PGR, CdS QD and CdS/Br-PGR composite material at 375 nm and shown in Figure 4. No luminescence was observed from the Br-PGR molecule after exciting at 375 nm, which might be due presence of multiple hydroxyl group adjacent to the phenyl ring that facilitate faster non-radiative decay process. Figure 4a shows photoluminescence spectra of the CdS QD in chloroform after exciting at 375 nm, which consists an emission peak at 452 nm with high emission quantum yield (ϕ_{CdS} = 36%). Figure 4b shows the emission spectra of CdS QD in the presence of 36 μM Br-PGR in chloroform solution. It is very interesting to see that the emission intensity of the CdS QD is drastically reduced in presence of Br-PGR molecule. Due to close proximity between QD and molecular adsorbate in the CdS/Br-PGR composite system one can envisage emission quenching might be due to energy transfer. To realize energy transfer it's very important to have overlap between QD luminescence and Br-PGR absorbance. It has been observed that there is some overlap between CdS luminescence and Br-PGR absorbance (Supporting Information). However no luminescence was observed from Br-PGR after exciting CdS in the CdS/Br-PGR composite system. Still we cannot rule out energy transfer process between CdS QD and Br-PGR. However, it is clearly seen from Scheme 1 that the VB (1.35 V versus NHE) of CdS lies below the HOMO (0. 458 V vs NHE) of Br-PGR, so the photo-excited hole in the valence band of CdS can be captured by Br-PGR, which is

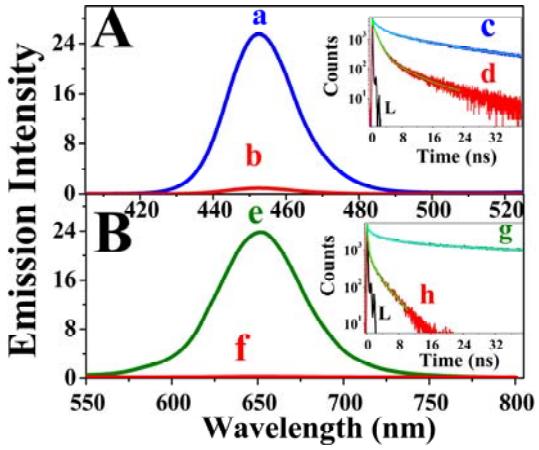

Figure 4: Panel A: Photoluminescence spectra of the CdS QD in absence (a) and in presence of Br-PGR (b) after exciting at 380 nm. **Inset**: Emission decay traces of the CdS QD (c) and CdS/Br-PGR (d) composite after exciting at 374 nm and monitoring at 452 nm. **Panel B:** Photoluminescence spectra of the CdS/CdTe QD in absence (e) and in presence of Br-PGR (f) after exciting at 500 nm. **(Inset)** Emission decay traces of the CdS/CdTe (g) and CdS/CdTe with Br-PGR (h) composite after exciting at 406 nm and monitoring at 650 nm. **L** is the excitation profile.

thermodynamically viable process. So the emission quenching can be attributed to hole transfer from photo-excited CdS to Br-PGR molecule. The hole-transfer reaction can be expressed by the equations below:

$$\mathbf{CdS + h\nu \rightarrow CdS\ (e^- + h^+)} \qquad \mathbf{(1)}$$

$$\mathbf{CdS\ (e^- + h^+) + Br\text{-}PGR \rightarrow CdS\ (e^-) + Br\text{-}PGR\ (h^+)} \qquad \mathbf{(2)}$$

Now to reconfirm the hole transfer process and to monitor hole transfer dynamics we have carried out time-resolved emission studies of pure CdS QD and also Br-PGR sensitized CdS QD and shown in Figure 4 inset. The emission decay traces of the CdS QD and CdS/Br-PGR composite have been monitored at 452 nm after exciting the samples at 374 nm laser excitation source. The emission decay traces for the CdS QD can be fitted multi-exponentially with time constants τ_1 = 0.951 ns (24.2%), τ_2 = 5.59 ns (29%), τ_3 = 23.11 ns (46.8%), with τ_{avg} =12.7 ns (Trace c Figure 4 A).

Here the short decay component (~0.951 ns) can assigned to the optically active $1S_e$–$1S_{3/2}$ exciton state. However the longer components, (~5.59) and (~23.11 ns) can be assigned to surface-trapped charge carriers and the dark exciton state in CdS QD[52]. Interestingly the emission decay traces for CdS/Br-PGR can be fitted multi-exponentially with time constants of

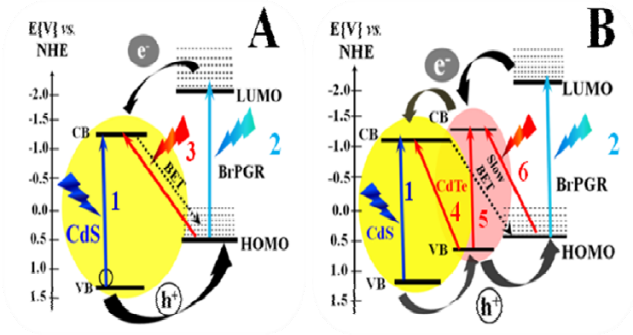

Scheme 1. Schematic diagram illustrating electron and hole transfer process in CdS QD (section A) and CdS/CdTe-Type-II core/shell QD (section B) sensitized by Br-PGR. **Process 1** shows excitation of CdS QD and whereas **Process 2** shows photo-excitation of Br-PGR. **Process 3** indicates direct transfer of electron from HOMO of Br-PGR to conduction band of CdS. **Process 4** shows indirect photo-excitation electron from valence band CdTe shell QD to conduction band of core CdS QD. **Process 5** shows photo-excitation of CdTe shell QD. **Process 6** indicates direct transfer of electron from HOMO of Br-PGR to conduction band of CdTe shell. Electron injection and hole transfer reaction in both composite materials are shown. Dotted line in both the scheme indicates charge recombination reaction between electron in CdS QD and Br-PGR cation radical. **BET** (back electron transfer) process is slower in case of CdS/CdTe-BrPGR composite system.

τ_1 = 0.16 ns (43.4%), τ_2 = 1.2 ns (51.1%), τ_3 = 5.78 ns (5.5%), with τ_{avg} =1 ns respectively (Trace trace d Figure 4 A). It is interesting to see that the average lifetime of the CdS/Br-PGR system is more than 12 times shorter as compared to that of CdS QD, which confirms a hole-transfer process in the composite materials, as suggested in equation 2. Presumably, the observed decrease in lifetime arises due to hole transfer (HT) from the CdS QD to Br-PGR molecule, and then, the hole-transfer rate constant can be determined through the following expression

$$\mathbf{k_{HT} = (1/\tau_{CdS/Br\text{-}PGR}) - (1/\tau_{CdS})} \qquad \mathbf{(3)}$$

Using the average lifetime values of 12.7 ns (CdS) and 1 ns (CdS/Br-PGR), the hole-transfer rate constant can be determined to be $9.2 \times 10^8\ s^{-1}$.

It has been observed that Br-PGR form strong charge transfer complex with CdS/CdTe which indicates that charge transfer takes place in the ground state itself. To corroborate charge transfer process in the excited state we have also carried out both steady state and time resolved emission studies type II (CdS/CdTe) core-shell in presence and absence of Br-PGR adsorbate molecule to monitor charge transfer process. Figure 4B depicts the photoluminescence spectra of CdS/CdTe type II core/shell in absence (trace e) and in presence (trace f) of Br-PGR molecule after exciting at 530 nm. No emission was observed for pure Br-PGR after exciting at 530 nm.
Exciting CdS/CdTe type II core/shell at 530 nm, luminescence was observed in 580 – 720 nm region with emission peak at 652 nm (with quantum yield $\phi_{CdS/CdTe}$ = 2.9%). This can be attributed to indirect band gap emission. Now in presence Br-PGR the indirect photoluminescence of the core/shell completely quenches. Energy transfer between photo-excited CdS/CdTe core-shell and Br-PGR can be rule out as there is no overlap between core-shell luminescence and Br-PGR absorbance (Supporting Information). So the emission quenching can be attributed purely due to hole transfer from CdTe to Br-PGR. The hole-transfer reaction can be expressed by the equations below:

$$\mathbf{CdS/CdTe + h\nu \rightarrow CdS\ (e^-) + CdTe\ (h^+)} \qquad \mathbf{(4)}$$

$$\mathbf{CdTe\ (h^+) + Br\text{-}PGR \rightarrow CdTe + Br\text{-}PGR\ (h^+)} \qquad \mathbf{(5)}$$

On photoexcitation of CdS/CdTe type II core shell, the photo-excited electron will be localized in conduction band of CdS core while hole will be localized in the valence band of CdTe shell (Scheme 1B). In presence of Br-PGR adsorbate photo-excited hole will be transferred to Br-PGR as the valence band of CdTe lies below the HOMO of Br-PGR (Scheme 1B). Now to verify the cascading charge transfer dynamics we have carried out time-resolved emission studies. Figure 4B inset shows the emission decay trace of CdS/CdTe core/shell in absence and in presence at 652 nm after exciting the samples at 406 nm laser excitation source. The emission decay trace for CdS/CdTe core/shell (Figure 4g) and CdS/CdTe core/shell with Br-PGR (Figure 4 h) can be fitted multiexponentially with time constants τ_1 = 0.17 ns (58%), τ_2 = 2.2 ns (21%), τ_3 = 19.8 ns (21%), with τ_{avg} =15 ns and τ_1 = 0.2 ns (89%), τ_2 = 1 ns (7%), τ_3 = 4.2 ns (4%), with τ_{avg} =0.42 ns. It is clearly seen that in presence of Br-PGR emission intensity drastically reduced which can be attributed due to hole transfer from photo-excited hole from type II core shell to Br-PGR where the hole transfer rate can be monitored by using the equation below and the hole transfer rate is measured to be $2.2 \times 10^9\ sec^{-1}$.

$$\mathbf{k_{HT} = (1/\tau_{CdS/CdTe\text{-}BrPGR}) - (1/\tau_{CdS/CdTe})} \qquad \mathbf{(6)}$$

Now, from Scheme 1, it is clear that a photoexcited Br-PGR molecule can inject an electron into the CB of CdS QD and in the CB of CdTe in CdS/CdTe type II core-shell. To observe this electron-transfer process from a photoexcited Br-PGR to CdS QD or CdS/CdTe core-shell it is important to monitor the emission from Br-PGR. However on exciting S1 state of Br-PGR no emission was observed and on exciting S2 state of Br-PGR negligible emission was observed which is too low to monitor electron injection dynamics on quantum dot surface. Now to monitor both electron injection and hole transfer dynamics in early time scale we have carried out femtosecond transient absorption spectroscopy and described in next section.

d) Femtosecond Transient absorption measurement study:

To corroborate charge (both electron and hole) transfer dynamics in early time scale with more accuracy in the above composite systems we have carried out femtosecond transient absorption spectroscopic measurements by exciting CdS/Br-PGR and CdS/CdTe/Br-PGR composite systems at 400 nm laser light. Before monitor the charge transfer dynamics of the above composite systems, it is very important to monitor excited state dynamics of the individual materials, CdS QD, CdS/CdTe core/shell and Br-PGR[51]. The excited state dynamics of the pure materials have been discussed in supporting information. Figure 5A shows the transient absorption spectra of photo-excited CdS/Br-PGR composite materials in different time delay, which includes a bleach below 650 nm with a maximum signal at 550 nm and a broad absorption band at above 700 nm to 800 nm region. The negative absorption below 650 nm appears due to bleach signal of ground state absorption of the CdS/Br-PGR complex and it matches with steady state absorption (Figure 3c). The broad spectral absorption in the 700-900 nm regions can be attributed to both Br-PGR cation radical and the electrons in the conduction band in CdS QD[26]. Assignment of Br-PGR cation radical has been made on the basis of the results obtained in separate pulse radiolysis experiments (Supporting Information), where Br-PGR$^{\bullet+}$ was generated selectively by the reaction of a $N_3^{\bullet}$ radical with Br-PGR molecule in N_2O^- saturated aqueous solution. Br-PGR cation radical band is not clear in the transient spectra due to huge overlap of ground state absorption bleach in the same spectral region. Now to understand the charge transfer dynamics in ultrafast time scale in CdS/CdTe core/shell sensitized with Br-PGR system femtosecond transient measurements have been carried out after exciting the composite material at 400 nm and monitoring the transients in the visible region and shown in Figure 5B. The transient spectra consist of a bleach below 700 nm

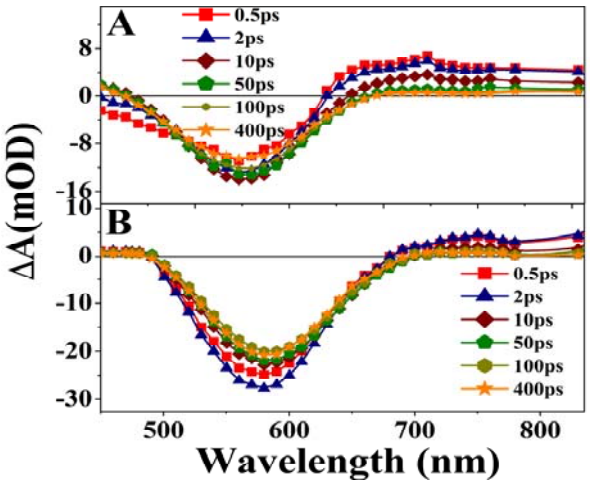

Figure 5: Transient absorption spectra of (A) CdS/Br-PGR and (B) CdS/CdTe-Br-PGR composite materials in chloroform at different time delay after excitation at 400 nm laser light.

with a maximum signal at 570 nm and a broad absorption band at above 700 nm to 900 nm region. In earlier section we have already mentioned that the positive absorption band is attributed to cation radical of Br-PGR and the conduction band electron of the quantum dot. The negative absorption below 700 nm can be attributed to bleach due to ground absorption of the CdS/CdTe+Br-PGR complex. Now it will be interesting to compare the spectral properties in both the above systems sensitized with Br-PGR. To compare transient spectral properties we would like to mention that we kept the same optical absorption (same O.D.) at 400 nm of the two composite mixtures. The negative absorption below 700 nm can be attributed to bleach due to ground absorption of the CdS/CdTe+Br-PGR complex. Now it will be interesting to compare the spectral properties in both the above systems sensitized with Br-PGR. The negative absorption below 700 nm can be attributed to bleach due to ground absorption of the CdS/CdTe+Br-PGR complex. Now it will be interesting to compare the spectral properties in both the above systems sensitized with Br-PGR. To compare transient spectral properties we would like to mention that we kept the same optical absorption (same O.D.) at 400 nm of the two composite mixtures.

It is clearly seen that in Figure 5 that the intensity of the transient bleach is almost two times higher in CdS/CdTe core-shell as compared to that of CdS QD after sensitizing with Br-PGR. Higher bleach intensity at the bleach wavelength for similar optical density at the exciting wavelength suggest better charge separation in CdS/CdTe/Br-PGR composite as compared to that in CdS/Br-PGR. Higher charge separation in core-shell might be due to result of cascading of electron and hole transfer after photo-excitation of the composite materials. Now to understand the charge transfer behaviour in these two systems the bleach kinetics are compared at 560 nm and 650 nm for CdS QD and CdS/CdTe core-shell sensitized with Br-PGR respectively and shown in Figure 6. The bleach kinetics for CdS/Br-PGR at 560 nm can be fitted with bi-exponential growth τ_1 = 150fs±20fs (84%) and τ_2 = 4.5 ps ±0.5ps (16 %) and multi-exponential decay with time constants of τ_1 = 56 ps ± 3 ps (24%), τ_2 = 300 ps ±15ps (28.5 %), and τ_3 > 1 ns ± 100ps (47.5%) (Table 1). However the bleach kinetics at 650 nm for CdS/CdTe/Br-PGR system can be fitted with single exponential growth of 150 fs ±

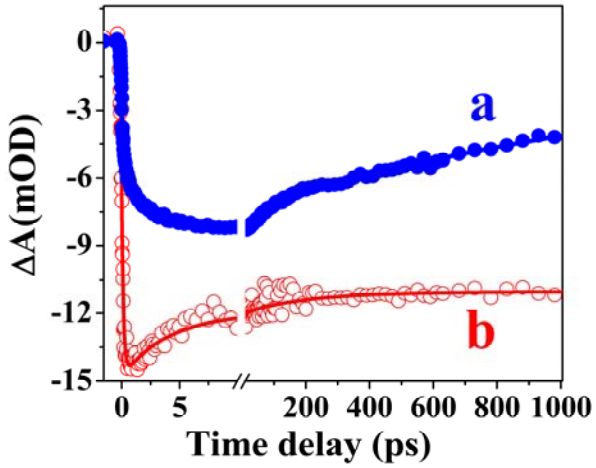

Figure 6. Normalized bleach recovery kinetic traces of (a) CdS QD sensitized Br-PGR at 560nm and (b) CdS/CdTe core/shell sensitized Br-PGR at 650nm in chloroform after exciting the samples at 400 nm laser light.

20 fs and multi-exponential decay time constants of τ_1= 4 ps ± 0.4ps (16%), τ_2 = 200 ps ± 20ps (7 %), and τ_3 > 1 ns ± 100ps (77%) (Table 1). The charge separation in both the above systems found to take place in three different path ways: through hole transfer from photo-excited QDs to BrPGR, electron injection from photo-excited BrPGR to CB of the QDs, and direct electron transfer from HOMO of BrPGR to the CB of the QDs. Due to overlap of transient absorption of cation radical of Br-PGR, electron in the conduction

of QD materials at the bleach wavelengths (560 nm and 650 nm) for both the above systems, it is very difficult to comments on different physical processes from the bleach recovery kinetics. Still we have tried to understand charge transfer dynamics from bleach kinetics in both the systems. It has been observed that growth kinetics at 560 nm can be fitted bi-exponentially. It is seen that at 400 nm for CdS/BrPGR system contribution due to CT complex is much less (Figure 3), as a result on photo excitation at 400 nm charge separation can take place mainly through hole transfer from QD to Br-PGR and through electron injection from photo-excited BrPGR to QDs. The faster growth component (150 fs) is attributed to electron injection from photo-excited BrPGR to Cds QD and slower bleach growth (4 ps) can be attributed to hole transfer process from CdS QD to Br-PGR. However in CdS/CdTe/Br-PGR system at 400 nm, absorption due to CT complex dominates over the absorption due to CdS/CdTe core-shell and Br-PGR. As a result charge separation can take place through direct electron transfer process from QDs to Br-PGR and electron injection from Br-PGR to QDs which takes place in <150 fs ±20 fs. In addition to the above two processes hole transfer from CdS/CdTe core-shell to Br-PGR also take place with ~4 ps, as determined from first bleach recovery time constant (Table 1). Now let us discuss the multi-exponential bleach recovery kinetics which can be attributed to recombination dynamics between Br-PGR cation radical and electron in CdS QD or CdS/CdTe core-shell of different trap depth or different distance (spatial distance) from cation radical. Main aim of this investigation is to demonstrate the effect of shell on charge recombination dynamics between electron in conduction band of QDs and cation radical which has been observed to be much slower in core-shell system as compared to without shell.

CdS/DBF composite materials where CdS and DBF form charge transfer complex and act as super-sensitizer in quantum dot solar cell. Similarly CdS/Br-PGR also can act as super senstizer where charge separation in the composite materials can take place in different path ways. From steady state and time-resolved emission measurements we have confirmed that photo-excited hole of CdS

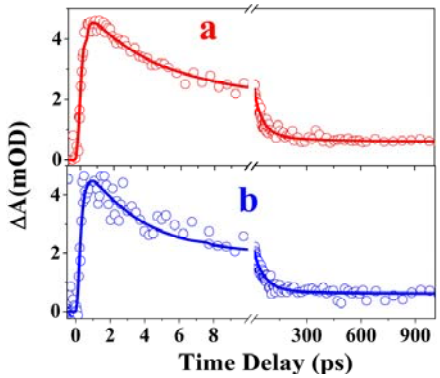

Figure 7. Transient absorption decay kinetics of a) CdS/Br-PGR complex and b) CdS/CdTe/Br-PGR complex at 780 nm after exciting the samples with 400nm laser light.

We have also monitored transient kinetics at 780 nm for both the above systems to monitor the injected electron in the QD and QD core-shell and are shown in Figure 7. It is interesting to see that in both the kinetics at 780 nm can be fitted with pulse-width limited growth and multi-exponential decay which can be fitted with time constants of τ_1 = 4 ps ±0.4ps (55%), τ_2 = 50 ps ± 5ps (32 %), and τ_3 > 1 ns ± 100ps (13%) for CdS/Br-PGR and τ_1 = 3 ps ±0.3ps (57%), τ_2 = 60 ps ± 5ps (29 %), and τ_3 > 1 ns ± 100ps (14%) for CdS/CdTe/Br-PGR systems respectively (Table 1). Here in both the systems the faster decay components (3-4 ps) at 780 nm can be attributed to electron trapping dynamics on QD and QD core-shell surface[13, 14, 53].

e) Charge Transfer Dynamics in quantum dot and type II core/shell quantum dot sensitized molecular adsorbate:

In steady state absorption studies we have observed that Br-PGR form strong charge transfer complex with both CdS QD and CdS/CdTe core-shell which suggest that in the ground state itself partial charge separation take place in both the systems. In our earlier studies we have demonstrated charge transfer dynamics in QD can be captured very efficiently by Br-PGR and from ultrafast transient absorption measurements we can see that charge separation can take place in multiple path ways and it has been demonstrated in Scheme 1. It is clearly seen that photo-excited Br-PGR can inject electron into the conduction band of CdS denoted as path 2 and direct electron transfer from HOMO of Br-PGR to the conduction band which we have termed as path 3. However in the present investigation charge transfer dynamics in CdS/CdTe/Br-PGR system is more complex as compared to that in CdS/Br-PGR system. On photo-excitation CdS/CdTe/Br-PGR system charge separation can take place in several path ways. After exciting CdS QD through path 1 hole can be transferred to CdTe shell which eventually can be captured by Br-PGR as shown in Scheme 1B. On the other hand photo excitation of Br-PGR (path 2) electron injection can take place to the conduction band of CdTe shell and eventually it will be transferred CdS core. We have already observed from steady and time-resolved absorption and emission studies that in CdS/CdTe type II core-shell that charge separation take place due to indirect band-gap excitation which we have denoted as path 4 in Scheme 1 B. Now on photoexcitation of CdTe shell electron and hole pair can be created through path 5 where electron can be transferred to CdS core and hole can be captured by Br-PGR. In addition to the above processes direct electron transfer also can take place from HOMO level of Br-PGR to conduction band of CdTe shell (path 6) and finally transferred to CdS core. From Scheme 1 it is clear that charge transfer dynamics in both the above systems are quite different and now it is important to monitor the charge recombination dynamics. Charge recombination dynamics between electron in CdS (both CdS QD and CdS/CdTe core-shell) and Br-PGR cation radical has been monitored from bleach recovery kinetics as shown in Figure 6. It is clearly seen that recombination dynamics is much slower in CdS/CdTe/Br-PGR system as compared to that in CdS/Br-PGR system. Slower charge recombination in CdS/CdTe core-shell was observed as compared to CdS QD due to spatial charge separation in type II arrangement. From the above experimental verification which includes steady state and time-resolved transient absorption and luminescence studies, it is quite clear that both the above systems are perfect composite materials for super sensitization in quantum dot solar cell. Both electron injection and hole transfer processes are facilitated due to type II core-shell arrangements and also these composite materials absorb more solar radiation as compared to that of the individual materials due to formation of strong charge transfer complex which absorb more light in the red region of the solar spectrum. This supersensitization scheme can bring significant improvement in QDSCs without changing the device fabrication much.

Table1. Parameters for multiexponential fit of transient kinetics of CdS/Br-PGR and CdS/CdTe-Br-PGR complex at different key wavelengths after excitation at 400nm laser light.

System	Wavelength (nm)	τ_{g1}	τ_{g2}	τ_1	τ_2	τ_3
CdS-BrPGR	560	150 fs ±20 fs (84%)	4.5 ps ±0.5ps (16%)	56 ps ± 3 ps (-24%)	300 ps±15ps (-28.5%)	>1ns ± 100ps (-47.5%)
CdS/CdTe-BrPGR	650	150fs ±20 fs (100%)		4 ps ±0.4ps (-16%)	200 ps±20ps (-7%)	>1ns ± 100ps (-77%)
CdS-BrPGR	780	150 fs ±20 fs (100%)		4 ps ±0.4ps (-55%)	50 ps ± 5ps (-32%)	>1ns ± 100ps (-13%)
CdS/CdTe-BrPGR	780	150fs ±20 fs (100%)		3 ps ±0.3ps (-57%)	60 ps ±5ps (-29%)	>1ns ± 100ps (-14%)

Conclusions

Ultrafast hole- and electron-transfer dynamics in the CdS QD, and CdS/CdTe type II core-shell sensitized with Br-PGR molecule have been demonstrated by using time-resolved emission and ultrafast transient absorption techniques, which suggests charge separation in both the composite materials take place in multiple pathways. Steady state optical absorption studies suggest Br-PGR form strong charge transfer complex with both CdS QD and CdS/CdTe core-shell which facilitate higher charge separation in the excited state. Photo-excitation of CdS/Br-PGR composite charge separation take place in different path ways like photo-excited hole transfer from CdS QD to Br-PGR, phtoexcited electron injection from Br-PGR to the conduction band of CdS QD and direct electron transfer from HOMO level of Br-PGR to the conduction band of CdS QD. However on photo-excitation of CdS/CdTe/Br-PGR composite material photo-excited hole from CdS core QD transfer to Br-PGR through valence band of CdTe shell and photo-excited Br-PGR inject electron into the conduction band CdTe shell QD which finally transferred to the conduction band of CdS core QD. In addition to that direct electron from HOMO of Br-PGR to conduction band of CdTe shell QD and CdS core QD take place. In all the above processes finally all the electrons are localized in core CdS QD and the holes are localized in Br-PGR with the formation of Br-PGR cation indicating huge spatial charge separation. Charge recombination dynamics in CdS/CdTe/Br-PGR system found to be much slower as compared to that in CdS/Br-PGR system. Our observation confirms the reality of multiple exciton dissociation and finally higher photoconversion efficiency in QDSCs through core-shell super-sensitization.

Acknowledgements

P.M. acknowledges DAE and T.D. acknowledge CSIR for research fellowship. This work was supported by "DAE-SRC Outstanding Research Investigator Award" (Project/Scheme No. : DAE-SRC/2012/21/13-BRNS) granted to Dr. H. N. Ghosh. We sincerely thank Dr. A. K. Tyagi, Chemistry Division, BARC for XRD measurement. We sincerely thank Dr. D. K. Palit and Dr. B. N. Jagatap for their encouragement.

Notes and references

Radiation and Photochemistry Division, Bhabha Atomic Research Centre, Mumbai-400085, India.

To whom correspondence should be addressed. E-mail: hnghosh@barc.gov.in, Fax: (+) 91-22-25505331/25505151

Electronic Supplementary Information (ESI) available: High resolution Transmission Electron Microscope (HRTEM) images of CdS QD and CdS/CdTe core-shell, Measurement of Emission Quantum Yield of the QD materials, Ultrafast transient absorption Studies of CdS quantum Dot CdS/CdTe type II core/shell and bromo-pyrogallol red (Br-PGR), Steady state absorption of Br-PGR and emission of CdS QD and CdS/CdTe core-shell and Transient absorption spectrum of cation radical of bromo-pyrogallol red (Br-PGR) (uncorrected) See DOI: 10.1039/b000000x/

References:

(1) P. V. Kamat, *J. Phys. Chem. Lett.*, 2013, **4**, 908.
(2) E. H. Sargent, *Nature photonics*, 2012, **6**,133.
(3) I. Mora-Sero and J. Bisquert, *J. Phys. Chem. Lett.*, 2010, **1**, 3046
(4) S. Rühle, M. Shalom, and A. Zaban, *Chem. Phys.Chem.*, 2010, **11**, 2290.
(5) J. Wang, I. Mora-Sero, Z. Pan, K. Zhao, H. Zhang, Y. Feng, G. Yang, X. Zhong and J. Bisquert, *J. Am. Chem. Soc*., 2013, **135**, 15913.
(6) F. Hetsch, X. Xu, H.Wang, S. V. Kershaw and A. L. Rogach, *J. Chem. Phys. Lett.*, 2011, **2**, 1879.
(7) I. Hod, and A. Zaban, *Langmuir*, 2014, **30**, 7264.
(8) J. T. Stewart, L. A. Padilha, W. K. Bae, W. K. Koh, J. M. Pietryga and V. I. Klimov, *J. Phys. Chem. Lett.*, 2013, **4**, 2061.
(9) J. E. Murphy, M. C. Beard, A. G. Norman, S. P. Ahrenkiel, J. C. Johnson, P.Yu, O. I.Micic, R. J. Ellingson and A. J. Nozik, *J. Am. Chem. Soc.*, 2006, **128**, 3241.
(10) J. M. Luther, M. C. Beard, Q. Song, M. Law, R. J. Ellingson and A. J. Nozik, *Nano Lett.* ,2007, **7,** 1779.
(11) V. I. Klimov, *Annu. Rev. Phys. Chem.*, 2007, **58**, 635.
(12) M. C. Beard, J. M. Luther, O. E. Semonin, and A. J. Nozik, *Acc. Chem. Res.*, 2013, **46**, 1252.
(13) P. Kambhapati, *Acc. Chem. Res.*, 2011, **44**, 1.
(14) S. L. Sewall, R. R. Cooney, K. E. H. Anderson, E. A. Dias, D. M. Sagar, and P. Kambhampati, *J. Chem. Phys.*,2008, **129**, 084701.

(15) J. A. Chang, S. H. Im, Y. H. Lee, H.J. Kim, C. S. Lim, J. H. Heo and S. I. Seok, *Nano Lett.*, 2012, **12**, 1863.
(16) Z. X. Pan, K. Zhao, J. Wang, H. Zhang, Y. Y. Feng and X. H. Zhong, *ACS Nano*, 2013, **7**, 5215.
(17) P. K. Santra and P. V. Kamat, *J. Am. Chem. Soc.*, 2012, **134**, 2508.
(18) S. Mathew, A. Yella, P. Gao, B. R. Humphry, B. F. E. Curchod, N. A. Astani, I. Tavernelli, U. Rothlisberger, M. K. Nazeeruddin, and M. Graötzel, *Nature Chemistry*, 2014, **6**, 242.
(19) A. J. Nozik, *Annu. Rev. Phys. Chem.*, 2001, **52**, 193.
(20) P. V. Kamat, A. Jeffrey. Christians and J. G. Radich, *Langmuir*, 2014, **30**, 5716.
(21) N. Song, H. Zhu, S. Jin and T. Lian, *ACS nano*, **2011**, *5*, 8750
(22) I. Robel, M. Kuno and P. V. Kamat, *J. Am. Chem. Soc.*,2007, **129**, 4136.
(23) Y. Yang, W. Rodríguez-Córdoba, X. Xiang and T.Lian, *Nano Lett.*, 2012, **12**, 303.
(24) J. Huang, Z. Huang, Y. Yang, H. Zhu and T. Lian, *J. Am. Chem. Soc.*, 2010**, 132**, 4858.
(25) A. J. Morris-Cohen, M. T. Frederick, L. C. Cass and E. A. Weiss, *J. Am. Chem. Soc.*, 2011, **133**, 10146.
(26) P. Maity, T. Debnath and H. N. Ghosh, *J. Phys. Chem. Lett.*, 2013, **4**, 4020.
(27) P. Singhal and H. N. Ghosh, *J. Phys. Chem. C*, 2014, **118**, 16358.
(28) T. Debnath, P. Maity and H. N. Ghosh, *Chem. Eur. J.*,2014, **20**, 13305.
(29) T. Debnath, P. Maity, S. Maiti and H. N. Ghosh, *J. Phys. Chem. Lett.*, 2014, **5**, 2836.
(30) H. Choi and P. V. Kamat, *J. Phys. Chem. Lett.*, 2013, **4**, 3983.
(31) C-H. Chuang, S. S. Lo, G. D. Scholes and C. Burda, *J. Phys. Chem. Lett.*, 2010, **1**, 2530.
(32) S. Kim, B. Fisher, H-J. Eisler and M. Bawendi, *J. Am. Chem. Soc.*,2003, **125**, 11466.
(33) M. Okano, M. Sakamoto, T. Teranishi, and Y. Kanemitsu, *J. Phys. Chem. Lett.*, 2014, **5**, 2951.
(34) Q. H. Zeng, X. G. Kong, Y. J. Sun, Y. L. Zhang, L. P. Tu, J. L. Zhao and H. Zhang, *J. Phys. Chem. C*, 2008, **112**, 8587.
(35) X. Ma, A. Mews and T. Kipp, *J. Phys. Chem. C*, 2013, **117**, 16698.
(36) M. Sakamoto, K. Inoue, M. Saruyama, Y-Gi. So, K. Kimoto,M. Okano, Y. Kanemitsua and T. Teranishi, *Chem. Sci.*, 2014, **5**, 3831.
(37) H. Zhong, Y. Zhou, Y. Yang, C. Yang and Y. Li, *J. Phys. Chem. C*, 2007, **111**, 6538.
(38) S. Rawalekar, S. Kaniyankandy, S. Verma and H. N. Ghosh, *J. Phys. Chem. C*, 2010, **114**, 1460.
(39) Y. Nonoguchi, T. Nakashima and T. Kawai, *Small,* 2009, **5**, 2403.
(40) D. Zhao, Z. He, W. H. Chan and M. M. F. Choi, *J. Phys. Chem. C*, **2009, 113**, 1293.
(41) Y. Yan, G. Chen and P. G.V. Patten, *J. Phys. Chem. C,* 2011, **115**, 22717.
(42) X.Y. Yu, B.X. Lei, D.B. Kuang, and C.Y. Su, *Chem. Sci*., 2011, **2**, 1396.
(43) J. H. Bang and P. V. Kamat, *ACS Nano,* 2009, **3**, 1467.
(44) L. Etgar , D. Yanover , R. K. Capek, R. Vaxenburg, Z. Xue, B. Liu , Nazeeruddin M. K., E. Lifshitz and M. Grätzel. *Adv. Funct. Mater.*, 2013, **23**, 2736.
(45) H. Zhu, N. Song, W. Rodríguez-Córdoba and T.Lian, *J. Am. Chem. Soc.*, 2012, **134**, 4250.
(46) K. Wu, N. Song, Z. Liu, H. Zhu, W. Rodríguez-Córdoba and T. Lian, *J. Phys. Chem. A*, **2013**, **117**, 7561.
(47) H. Zhu, N. Song and T. Lian, *J. Am. Chem. Soc.*, 2010, **132**, 15038.
(48) W. W. Yu, L. Qu, W. Guo and Xi.Peng, *Chem. Mater.,* 2003, **15**, 2854.
(49) Z. Deng, O. Schulz, S. Lin, B. Ding, X. Liu, X. Wei, R. Ros, H. Yan and Y. Liu, *J. Am. Chem. Soc.,* 2010, **132**, 5592.
(50) H. Choi, R. Nicolaescu, S. Paek, J. Ko and P. V. Kamat, *ACS Nano,* 2011, **5**, 9238.
(51) G. Ramakrishna, H. N. Ghosh, A. K. Singh, D. K. Palit and Mittal, J. P. *J. Phys. Chem. B,* 2001, 105, 12786.
(52) S. Verma, S. Kaniyankandy and H. N. Ghosh, *J. Phys. Chem. C,* 2013, **117**, 10901.
(53) P. Tyagi, and P. Kambhampati, *J. Chem. Phys.*, 2011, **134**, 094706.